Ageostrophic Winds Associated with a Tropical Cyclone and Northward Moisture Fluxes

Kazuo Saito[1,2,3] and Takumi Matsunobu[4]

[1]Atmosphere and Ocean Research Institute/University of Tokyo, [2]Meteorological Research Institute, [3]Japan Meteorological Business Support Center, [4]University of Tsukuba

1. Background

In Japan, heavy rainfalls often occur when a typhoon exists off the south coast of Japan (Fig. 1). This phenomenon is often explained by northward moisture transport by a typhoon, however, 'northward' emission from typhoon violates the relationship of geostrophic wind:

$$u_g = -\frac{1}{f}\frac{\partial \phi}{\partial y}, v_g = \frac{1}{f}\frac{\partial \phi}{\partial x}.$$

These pre-typhoon rainfalls are also known in other countries and called as 'PRE' (Fig. 2). PRE is enhanced by deep poleward moisture transport ahead of the recurving TC (Schumacher et al. 2011).

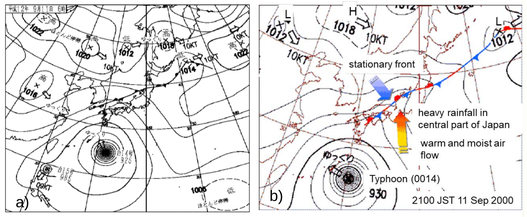

Fig. 1: a) Surface weather map at 2100 UTC Sep 10, 2000. b) Schematic explanation of the remote effect of the typhoon. After JMA homepage.

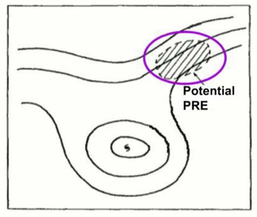

Fig. 2. Antecedent rainfall associated with TC. (Basart and Carr 1978; Cote 2007).

Ageostrophic winds were first discussed as a vertical circulation associated with a synoptic frontal zone. Near the baroclinic zone, the Sawyer (1952) and Eliassen's (1962) secondary circulation in the jet-streak four quadrant model is well known as the dynamical origin (Fig. 3a). Another topic on ageostrophic winds is the low-level jet (Fig. 3b). Diabatic heating by rainfall induces the pressure gradient force toward the mesoscale convective system. Vertical mixing and/or transport of horizontal momentum may also provoke ageostrophic winds.

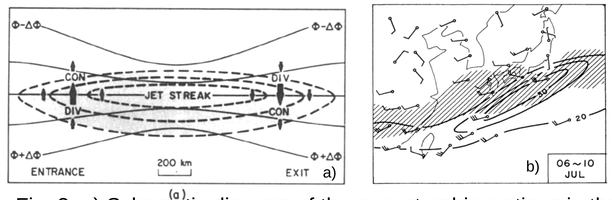

Fig. 3: a) Schematic diagram of the ageostrophic motions in the vicinity of straight jet-streak (Shapiro and Keyser 1990). b) 5-day mean 850 hPa wind field and mean heavy cloud zone (hatched) during in July 1968 (Akiyama1978).

2. Ageostrophic winds with Typhoon Melor (T0918)

Typhoon Melor (0918) made landfall in central Japan on 8 October 2009. Considerable rainfall was observed over southern part of Japan along a stationary front at the pre-typhoon period (Fig. 4). When the typhoon approached Japan, distinct ageostrophic southerly winds were observed over western part of Japan (Fig. 5).

References:

Saito, K., T. Fujita, Y. Yamada, J. Ishida, Y. Kumagai, K. Aranami, S. Ohmori, R. Nagasawa, S. Kumagai, C. Muroi, T. Kato, H. Eito and Y. Yamazaki, 2006: The operational JMA nonhydrostatic mesoscale model. *Mon. Wea. Rev.*, **134**, 1266-1298.

Saito, K., 2019: On the northward ageostrophic winds associated with a tropical cyclone. *SOLA*, **15**, 222-227.

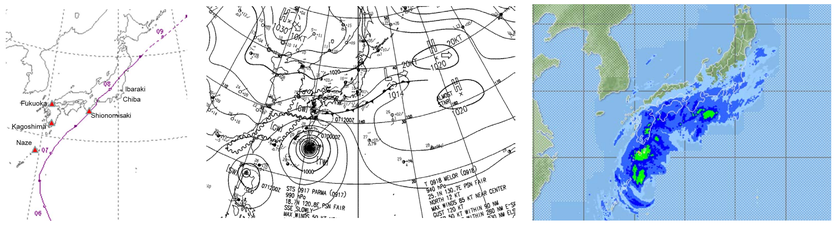

Fig. 4. a) Track of Typhoon Melor (0918). Numerals show the date and the positions of the typhoon center at 0000 UTC. Triangles indicate positions of aerological observatories. b) Surface weather map at 1200 UTC 6 October 2009. c) Precipitation analysis of JMA at 0000 UTC 7th October 2009.

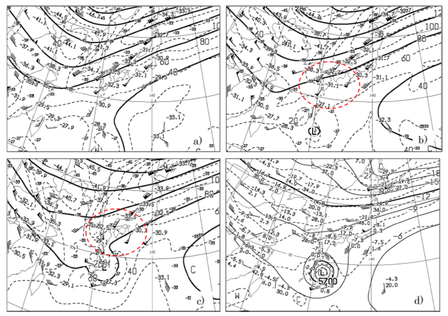

Fig. 5. a) Subjective analysis by JMA at 300 hPa level and observed winds at 0000 6 October 2009. b) Same as in a) but at 1200 UTC 6 October. Red ellipse by broken line indicates northward ageostrophic winds. c) Same as in a) but at 0000 UTC 7 October. d) Same as in c) but for 500 hPa.

3. Simulated northerly winds and discussion

The northerly ageostrophic winds were well simulated by JMA nonhydrostatic model (Fig. 6).

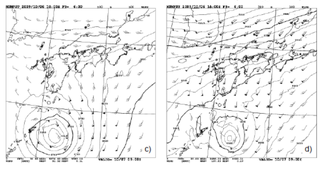

Fig. 6. a) Height field and horizontal winds at 500 hPa simulated by JMA-NHM for 00 UTC 7 October 2009 (FT= 6). b) Same as in b) but for 300 hPa

These ageostrophic winds are explained by a relationship between the horizontal velocity acceleration and the ageostrophic motion (Haltiner and Martin 1957).

$$\frac{du}{dt} = fv - \frac{\partial \phi}{\partial x} = f(v_a + v_g) - \frac{\partial \phi}{\partial x} = fv_a, \qquad (2)$$

$$\frac{dv}{dt} = -fu - \frac{\partial \phi}{\partial y} = -f(u_a + u_g) - \frac{\partial \phi}{\partial y} = -fu_a. \qquad (3)$$

When the contours around the TC are concentric circles (Fig. 7a), the pressure gradient force changes the direction of the wind toward the TC center, and wind speed becomes smaller than that of the geostrophic wind (gradient wind). When the TC approaches a jet streak from south, the geostrophic wind in the northeast quadrant is decelerated thus the ageostrophic wind vector toward northeast.

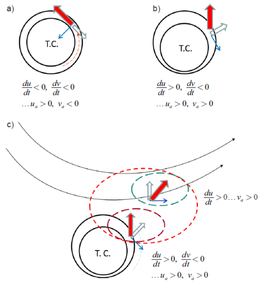

When a TC approaches a baroclinic zone (Fig. 7c) air mass is accelerated by the jet stream eastward, and the northward ageostrophic wind becomes positive. Consequently, when a TC approaches a baroclinic zone, southerly or southwesterly winds which cross the height contours prevail in the northeast of the TC.

Fig. 7. Relationship between height field (solid lines), acceleration vectors (blue thin arrows) and the ageostrophic wind components (double arrows).

As seen in Figs. 8a and 8b, areas of large northward winds are seen over main island of Japan and in the south of Kyushu and Shikoku. In the north east of the typhoon, ageostrophic winds are northeastward. A large positive northward ageostrophic wind area is seen over western Japan, corresponding to the eastward acceleration area. Sensitivity experiments revealed that contribution of the moist process is not primary to cause these ageostrophic winds (Saito 2019). Characteristic features of the non-axisymmetry of upper winds around a TC is also explained by the dynamically induced ageostrophic winds.

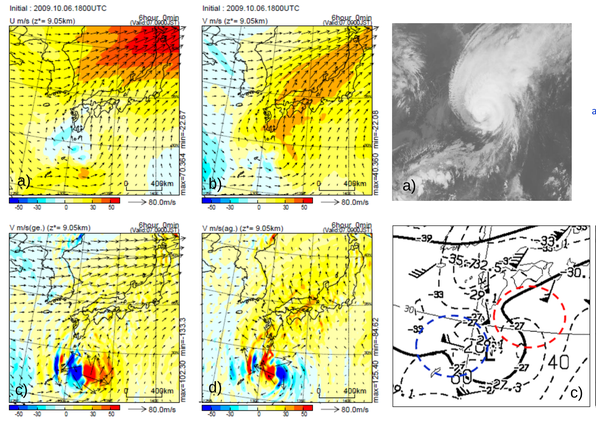

Fig. 8: a) Horizontal winds (vectors) and its u-component (color shade) at 300 hPa for 0000 UTC 7 October 2009 by JMA-NHM. b) Same as in a) but v-component of the horizontal wind. c) Geostrophic winds (vectors) and its v-components (color shade). d) Ageostrophic winds (vectors) and its v-components (color shade).

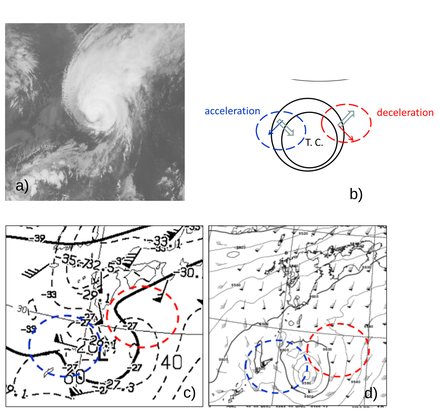

Fig. 9. a) MTSAT-1R infrared satellite images for 0000 UTC 7 October 2009. b) Relationship between the acceleration vector and ageostrophic wind including the north-western quadrant. c) Enlarged view of Fig. 2c. d) Enlarged view of Fig. 3d.

4. Northward moisture fluxes by ageostrophic winds

To evaluate the influence of the ageostrophic wind on PRE, we checked northward moisture fluxes by horizontal winds and the ageostrophic winds contribution. Figures 10a and 10b show northward moisture fluxes around z=9 km (27th to 30th model levels) by horizontal and ageostrophic winds. Ageostrophic winds apparently enhance the moisture fluxes over the western Japan. Although the northward ageostrophic winds are remarkable in the upper levels (red line in Fig. 10d), ageostrophic wind components contribute to enhance the deep poleward water vapor transport in middle and upper layers above 3 km (black line in Fig. 10d). In case when the low level jet exists, this mechanism may act even in the lower troposphere.

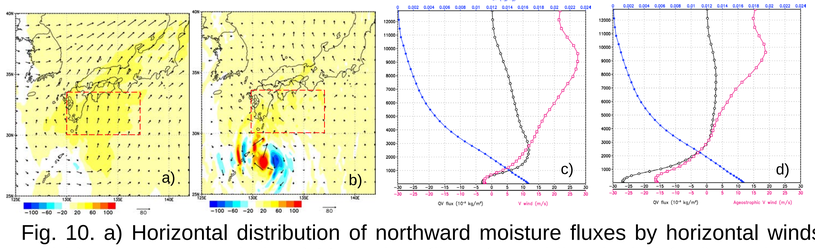

Fig. 10. a) Horizontal distribution of northward moisture fluxes by horizontal winds and b) ageostrophic winds. c) Vertical profiles of meridional wind (red), northward moisture fluxes (black) and water vapor over a red broken rectangle area (130-137 E, 30-33 N). d) Same as in the left figure but for ageostrophic components.